Artificial intelligence-based patient positioning for faster, more accurate and efficient CT imaging for COVID-19 patients

Yadong Gang
Zhongnan Hospital of Wuhan University
Xiongfeng Chen
Puren Hospital affiliated to Wuhan University of Science and Technology
Huan Li
Zhongnan Hospital of Wuhan University
Hanlun Wang
Zhongnan Hospital of Wuhan University
Jianying Li
Computed Tomography Research Center
Ying Guo
Computed Tomography Research Center
Junjie Zeng
Zhongnan Hospital of Wuhan University
Qiang Hu
Zhongnan Hospital of Wuhan University
Jinxiang Hu
Zhongnan Hospital of Wuhan University
Haibo Xu (xuhaibo1120@hotmail.com)
Zhongnan Hospital of Wuhan University

Research Article

Keywords: COVID-19, artificial intelligence, chest CT, radiation dose, image quality

Posted Date: August 12th, 2020

DOI: https://doi.org/10.21203/rs.3.rs-57162/v1

Version of Record: A version of this preprint was published at European Radiology on March 19th, 2021. See the published version at https://doi.org/10.1007/s00330-020-07629-4.

Abstract

Objective: To analyze and compare the imaging workflow, radiation dose and image quality for COVID-19 patients examined using either the conventional manual positioning method or an AI-based positioning method.

Materials and Methods: 127 adult COVID-19 patients underwent chest CT scans on a CT scanner using the same scan protocol except with the manual positioning (MP group) for the initial scan and an AI-based positioning method (AP group) for the follow-up scan. Radiation dose, patient off-center distance, examination and positioning time of the two groups were recorded and compared. Image noise and signal-to-noise ratio (SNR) were assessed by three experienced radiologists and were compared between the two groups.

Results: The AP group reduced the total positioning time and examination time by 28% and 8%, respectively compared with the MP group. Compared with the MP group, AP group had significantly less patient off-center distance (AP:1.56cm ± 0.83 vs. MP: 4.05cm ± 2.40, p<0.001) and higher proportion of positioning accuracy (AP: 99% vs. MP: 92%), resulted in 16% radiation dose reduction (AP: 6.1mSv ± 1.3 vs. MP: 7.3mSv ± 1.2, p<0.001) and 9% image noise reduction in erector spinae and lower noise and higher SNR for lesions in the pulmonary peripheral areas.

Conclusion: The AI-based positioning and centering in CT imaging is a promising new technique for reducing radiation dose, optimizing imaging workflow and image quality in imaging the chest. This technique has important added clinical value in imaging COVID-19 patients to reduce the cross-infection risks.

Key Points

1. The AI-based positioning (AP) method reduced the total positioning time and examination time by 28% and 8%, respectively compared with the manual positioning (MP).
2. AP had less patient off-center distance and higher proportion of positioning accuracy, resulted in 16% radiation dose reduction and 9% image noise reduction in erector spinae.
3. AP resulted in 9% image noise reduction and 15% SNR improvement for lesions in the pulmonary peripheral areas.

Summary Statement

AI-based positioning results in less radiation dose, and both higher examination efficiency and image quality in chest imaging, which added clinical value for diagnosing COVID-19 patients to reduce the cross-infection risks.

Introduction

Accurate patient positioning and centering in computed tomography (CT) remains an important issue of concern for reducing dose and image noise[1-3]. It was reported that the miscentered by 6 cm, resulting in up to 41% surface dose and 22% image noise increase[4]. To achieve high diagnostic image quality at reduced radiation dose, technologists make an extra effort to accurately select the anatomic scan range and carefully center the patients during CT scans. However, manual positioning and centering are a time-consuming process, and are technologist-dependent and often inconsistent and non-optimal, as well as of the potential cross-infection risk.

Recent advances in artificial intelligence (AI) technologies have demonstrated remarkable progress in recognizing and interpreting complex patterns in imaging data. The combination of AI and CT imaging can provide faster, more accurate and efficient imaging-based diagnosis[5]. By virtue of visual sensors, AI can identify the pose and shape of patients and realize an automated contactless image acquisition workflow. Yang Wang et al. (2020) reported that U-HAPPY (United imaging Human Automatic Planbox for PulmonarY) CT has a function with automatic positioning and scanning, which helps to reduce the radiation dose[6]. Recently, GE Healthcare also introduced a Revolution Maxima CT, which relies on deep learning algorithms and real-time depth sensing technology to center patients, locate desired anatomies and perform scan automatically. This CT scanner was successfully used for diagnosing COVID-19 patients in our hospital during the pandemic. However, applying AI to CT scanning technique is still at the exploratory stage, and to our knowledge, no previous research has compared the difference between the conventional manual positioning and centering method and AI-based positioning and centering method in detail. The purpose of this study was to analyze and compare the imaging workflow, radiation dose and image quality of COVID-19 patients who underwent several follow-up CT scans using the same CT protocol on a same CT machine but with either the conventional manual positioning mode or an AI-based positioning mode. We hope our findings may provide useful information on the characteristic of intelligent CT tools and help radiologists to achieve better images at the lower radiation dose more efficiently, while to reduce the risk of potential exposures. This study could prove to be the basis for the development of further intelligent imaging technology.

Materials And Methods

The research was approved by Medical Ethical Committee (Approved Number. 2020037). Our institutional review board waived written informed consents for this retrospective study.

Patients and data source

All the patients in our study had been diagnosed of COVID-19 according to the guideline of 2019-nCoV (Fifth Trial Edition) issued by the National Health Commission of China [7]. A total of 127 patients (68 men and 59 women; mean age, 57.7 years; age range, 20-83 years) with confirmed SARS-CoV-2 were identified who had undergone at least two chest CT studies at Wuhan Leishenshan Hospital between Feb 12, 2020 and Apr 10, 2020 (see more details in Table 1). These patients underwent the first chest CT using the conventional manual positioning and centering method, and an AI-based positioning and

centering method in the follow-up CT examination. Based on the different positioning methods, patients were categorized into the conventional manual positioning (MP) group and AI-based positioning (AP) group.

CT image acquisition and reconstruction

The imaging workflows for MP and AP groups are shown in Figure 1. A and B. The chest CT scanning was performed on a Revolution Maxima CT equipped with an AI-based automatic patient centering and anatomic positioning software (GE Healthcare, Waukesha USA) from the apex pulmonis to septum transversum. the AI-based positioning function uses the anatomical references and the scout range information to determine the landmark and the scan start and stop locations (Supplementary Fig 2). Both groups used the same scan protocol with the following parameters: tube voltage, 120 kVp; gantry rotation time, 0.4 second; pitch, 1.375:1; scan field-of-view (SFOV), 50cm; slice thickness, 5 mm; tube current (mA), automated tube current modulation (ATCM) to obtain a noise index of 11.57; All axial images were reconstructed using a standard reconstruction algorithm with the standard kernel; reconstruction display field-of-view (DFOV), 35-50 cm; reconstruction thickness, 1.25 mm.

Assessment of image quality

The image quality was analyzed by three radiologists (H.B.X., J.X.H., Y.D.G) at a standard pulmonary display window setting (window level, −700 and window width, 1500). Decisions were reached by consensus. The mean CT value and standard deviation (SDev) in Hounsfield Units (HU) of the aorta, trachea and erector spinae in the upper and middle thorax areas were measured by placing a 50 mm^2 region-of-interest (ROI) on a homogeneous-appearing area of these structures, as is shown in Figure 5. A, B. Three consecutive images were measured in each ROI area for each study, and the average value was determined. The mean and SDev of CT values within pulmonary lesions were also measured according to the method described above. The pulmonary lesions mainly included ground glass opacification, consolidation opacification and interstitial thickening (Fig 2). The pulmonary segments are defined by referring to the branching patterns of bronchi [8-10]. If a lesion was located in the outer one third of the lung, it was defined as peripheral, otherwise, it was defined as central. The signal-to-noise ratio (SNR) of the lesions was calculated based on the formula: SNR = Mean CT values/$SDev$. The image noise was represented using the SDev value.

Examination and positioning time

Total examination time and positioning time were recorded by the CT technologist for each study. The total examination time was defined as the time from the patient entering the CT scanning room to walking out of the exam room after finishing the CT examination. The positioning time was defined as the time from the patient lying on CT examination bed to technologist finishing positioning and starting scanning.

Radiation dose

The volume CT dose index ($CTDI_{vol}$ in mGy) and dose length product (DLP in mGy-cm) were recorded from the dose report image by the CT technologist for each study. The effective dose (ED in mSv) of the patient was calculated based on the formula: $ED = DLP \times C_f$, where the C_f represents the conversion factor for chest CT (C_f=0.014mSv/mGy-cm).

Off-center distance and positioning Accuracy

The patient off-center distance was measured using an axial CT image in the following steps: (1) select a transverse image containing manubrium and draw a horizontal line that passes through both armpits. (2) locate the center of the display field of view (DFOV) for the image. (3) record the vertical distance from the center of DFOV to the horizontal line. The vertical distance represented the patient off-center distance (Supplementary Fig 1. A). For the positioning accuracy, a complete coverage should contain the apex pulmonis to septum transversum. thus, if the images of apex pulmonis and septum transversum were fully covered, the patient positioning was considered successful, otherwise, it was defined incomplete or inaccurate.

Statistical analyses

Continuous variables were expressed as mean ± SD and compared using paired-sample *t* tests when the data were normally distributed; otherwise, the Wilcoxon signed-rank tests was used; The categorical variables were expressed as number (percentage %) and compared with McNemar's test. A two-tailed *P* value of less than 0.05 was considered statistically significant. All statistical analyses were conducted with IBM SPSS software (version 22.0).

Results

Baseline characteristics of objects

A total of 127 COVID-19 patients with a mean age of 57.7 years (year range 20 – 83 years) were included in our study. Among them, there were 68 (53.5 %) men and 59 (46.5 %) women. The ratio of man to woman was 1.15:1. Their body mass index (BMI) values were in the range of 17.4-33.1 kg/m^2, with an average value of 24.3 kg/m^2 (See Table 1).

Total examination time and positioning time

The total examination time and positioning time in the AP group were both significantly shorter than the MP group: the mean total examination time, AP: 120.0 s ± 21.0 vs. MP: 131.0 s ± 31.0, p=0.003; and the mean positioning time, AP: 29.0 s ± 7.0 vs. MP: 40.0 s ± 11.0, p<0.001, showed in Figure 1, C and D.

Positioning accuracy and off-center distance

The positioning accuracy and off-center distance were determined using patient chest CT images. A significantly higher positioning accuracy was recorded in the AP group (126 of 127, 99.0 %) than in the

MP group (117 of 127, 92.0 %) (Fig 3. C). The patient off-center distances obtained with the AI-based method were all significantly less than those obtained with the manual method (mean off-center distance: 1.56cm ± 0.83 in the AP group vs. 4.05cm ± 2.40 in the MP group, p<0.001) (Supplementary Fig 1).

Radiation dose

The AI-based positioning group had significantly lower CTDIvol value (13.3mGy ± 2.4 vs. 14.9mGy ± 2.3, p<0.001), DLP value (437.4mGy.cm ± 95.6 vs. 523.4mGy.cm ± 87.7, p<0.001) and ED value (6.1mSv ± 1.3 vs. 7.3mSv ± 1.2, p<0.001) than the manual positioning group (Fig 4).

Image noise and SNR

The image noise was represented by the SD measurement of the erector spinae in the upper and middle thorax areas. In both areas, the noise levels in CT images obtained with the AP method were all statistically lower than those in CT images obtained with the MP method: mean noise in the upper thorax, AP: 49.7HU ± 7.3 vs. MP: 54.1HU ± 9.3; and mean noise in the middle thorax, AP: 48.9HU ± 8.5 vs. MP: 53.9HU ± 9.1, (both p<0.001) (Fig 5, C and D). However, there was no significant differences for the noise values of the aorta and trachea in both groups.

Noise and SNR of pulmonary lesions

The pulmonary lesions could be found in any pulmonary segments in both groups. However, they predominantly distributed in the peripheral area of the lungs (766 of 791 lesions in the MP group, vs. 927 of 957 lesions in the AP group) (Table 3). Overall, the AP group had marginally lower image noise and higher SNR for the lesions from the pulmonary segment point of view (Table 2). But for lesions located in the peripheral area, the AP group had significantly lower noise and higher SNR than the MP group (Table 3).

Discussion

We analyzed and compared the imaging workflow, radiation dose and image quality for COVID-19 patients examined using either the conventional manual positioning method or an AI-based automatic patient positioning and centering method. Our results indicated that the AI-based method not only reduced the patient examination time, but also reduced the radiation dose to patients and overall image noise by better positioning and centering the patients.

Achieving high image quality at reduced radiation dose is always desirable. Reducing patient examination time and quickly diagnose becomes even more necessity during the COVID-19 pandemic, because quickly screening and treatment the patients should be the most critical measures for the control against this epidemic. Introducing artificial intelligence into CT imaging provides us a new way to achieve it. The auto-positioning function automatically detects an anatomical landmark by deep learning algorithms and allows minimizing positioning action into a single click operation, as illustrated in

supplementary figure 2. This automatic positioning operation was approved to be efficient in our research, which plays an essential role in helping the response to the COVID-19 pandemic. Our results showed that the use of AI-based positioning for chest CT scanning resulted in a shorter time to complete patient positioning and CT examination. In particular, the chest positioning time and total examination time were reduced in the AP group by 27.5% and 8.4%, respectively, as compared with the MP group. This automatic positioning operation was also approved to be accurate in our study. In our study, only one patient (1 out of 127) in the AP group required minor manual adjustment for the scan range after the AI selection. In addition, the scan range was more precise and was reduced by 6% overall based on the DLP report in the AP group which contributed to the additional 6% dose reduction for the patients in the AP group.

According to some related researches, off-center positioned patients substantially increase image noise and dose requirement[11]. In the AI-based patient positioning and centering technique, the 3D camera detects a depth information of patients and calculates the required table elevation to set the centering in the selected protocol. The auto centering function optimizes the radiation dose and image quality without of regard to operator's skill variance. Our research found that the patient off-center distances with the manual positioning method were more than those with the AI-based method. In our study, the patient off-center distance was substantially reduced from the 4.05cm ± 2.40 in the MP group to 1.56 cm ± 0.83 in the AP group. The off-center position reduction in the AP group subsequently reduced the radiation dose (CTDI) requirement to achieve similar image noise by 11%. Together with the tightened scan range brought about with the AI-based positioning, we achieved 16% dose reduction in the AP group (AP: 6.1mSv ± 1.3 vs. MP: 7.3mSv ± 1.2).

When patients are mispositioned in the gantry, not only the radiation dose requirement is artificially increased, the image quality often underperforms as well [12]. Our results also indicated that the noise level in CT images obtained with AP mode, particularly in the erector spinae and the lesions in the peripheral lung regions, were statistically lower than those in CT images obtained with MP mode. Chung et al. [13] reported that the lung lesions in COVID-19 patients are predominantly distributed in the peripheral region of the lungs. Hence the centered patients with AP mode may have the positive impact on image quality of peripheral lesions and provide potential dose reduction opportunities.

Recently, Yang Wang et al. reported the use of an intelligent system (U-HAPPY CT)[6] to reduce radiation exposure in chest CT application. Our results showed very similar radiation exposure reduction findings. In addition, we also demonstrated that the AI-based patient positioning and centering technique had the ability to reduce examination and positioning time and improve image quality.

Our research had some limitations. Firstly, our study may suffer from confounding bias due to the relatively small number of patients. Secondly, we only evaluated one CT scanner from one manufacturer. Additional studies are needed to investigate the generality of AI positioning on different CT scanners. Thirdly, Although the measurements in this study were performed on the same machine in the same

patient, there were still differences in the status of the patient compliance during the two CT examinations.

In summary, our study indicates that the use of AI-based patient positioning and centering results in less radiation dose, higher examination efficiency, higher positioning accuracy and higher image quality in imaging the chest. This technique has important added clinical value for diagnosing COVID-19 patients to reduce the cross-infection risks.

Declarations

Acknowledgments:

This study was supported by the National Key Research and Development Plan of China (Grants No. 2017YFC0108803), the National Natural Science Foundation of China (Grants No. 81771819 and No. 81801667). We thank Yunxiao Han and Yinghong Ge for assistance with the collecting image data. We thank Shuai Zhang, Zhusha Wang, Chenhong Fan, Wenbo Sun, Gao Lei and other members of the Department of Radiology, Zhongnan Hospital of Wuhan University for their help with comments and advice for revising the manuscript. Guarantors of integrity of entire study, Haibo Xu, MD, PhD and Yadong Gang, PhD.

Conflict of interest:

The authors of this manuscript declare no relationships with any companies, whose products or services may be related to the subject matter of the article. The authors declare that there are no conflicts of interest related to this article.

Abbreviations

Artificial intelligence = AI

2019 coronavirus disease = COVID-19

Manual positioning = MP

AI-based positioning = AP

Signal-to-noise ratio = SNR

References

1. Marsh RM, Silosky MS (2017) The effects of patient positioning when interpreting CT dose metrics: a phantom study. Med Phys 44(4):1514-1524. doi: 10.1002/mp.12137

2. Ohno Y, Koyama H, Seki S, Kishida Y, Yoshikawa T (2019) Radiation dose reduction techniques for chest CT: Principles and clinical results. Eur J Radiol 111:93-103. doi: 10.1016/j.ejrad.2018.12.017
3. Saltybaeva N, Alkadhi H (2017) Vertical off-centering affects organ dose in chest CT: evidence from Monte Carlo simulations in anthropomorphic phantoms. Med Phys 44(11):5697-5704. doi:10.1002/mp.12519
4. Toth T, Ge Z, Daly MP (2007) The influence of patient centering on CT dose and image noise. Med Phys 34(7):3093-3101. doi:10.1118/1.2748113
5. Shi F, Wang J, Shi J et al. (2020) Review of artificial intelligence techniques in imaging data acquisition, segmentation and diagnosis for covid-19. IEEE Rev Biomed Eng. doi: 10.1109/RBME.2020.2987975
6. Wang Y, Lu X, Zhang Y et al. (2020) Precise pulmonary scanning and reducing medical radiation exposure by developing a clinically applicable intelligent CT system: Toward improving patient care. EBioMedicine 54:102724. doi: 10.1016/j.ebiom.2020.102724
7. China National Health Committee (2020) Diagnosis and treatment of pneumonitis caused by novel coronavirus (trial fifth edition). China National Health Commission, China.http://www.nhc.gov.cn/xcs/zhengcwj/202003/46c9294a7dfe4cef80dc7f5912eb1989.shtml. Accessed 4 Feb 2020
8. Foster-Carter A, Hoyle C (1945) The segments of the lungs; a commentary on their investigation and morbid radiology. Dis Chest 11(6):511-564.doi: 10.1378/chest.11.6.511
9. Sealy WC, Connally SR, Dalton ML (1993) Naming the bronchopulmonary segments and the development of pulmonary surgery. Ann Thorac Surg 55(1):184-188. doi: 10.1016/0003-4975(93)90507-e
10. Ugalde P, de Jesus Camargo J, Deslauriers J (2007) Lobes, fissures, and bronchopulmonary segments. Thorac Surg Clin 17(4):587-599. doi: 10.1016/j.thorsurg
11. Szczykutowicz TP, DuPlissis A, Pickhardt PJ (2017) Variation in CT number and image noise uniformity according to patient positioning in MDCT. AJR Am J Roentgenol 208(5):1064-1072. doi: 10.2214/AJR.16.17215
12. Habibzadeh M, Ay MR, Asl AK, Ghadiri H, Zaidi H (2012) Impact of miscentering on patient dose and image noise in x-ray CT imaging: phantom and clinical studies. Phys Med 28(3):191-199. doi: 10.1016/j.ejmp.2011.06.002
13. Chung M, Bernheim A, Mei X et al. (2020) CT imaging features of 2019 novel coronavirus(2019-nCoV). Radiology 295(1):202-207. doi: 10.1148/radiol.2020200230

Tables

Table 1. Demographics and baseline characteristics of 127 COVID-19 patients included in this study.

Characteristics	Patients (*n*=127)
Age (years)	
Mean ± SD	58 ± 12
Range (years)	20 - 83
Sex	
male	68 (53.5%)
female	59 (46.5%)
Ratio of male to female	1.15:1
Body mass index (BMI, kg/m^2)	
Mean ± SD	24.3 ± 3.2
Range	17.4 - 33.1

Continuous value was presented as mean ± standard deviation (SD)

Table 2. Noise and SNC from pulmonary lesions with MP and AP on each pulmonary segment.

Location (Segment)	All lesions (*n*, MP/AP)	Noise		SNC		*P* value	
		MP	AP	MP	AP	Noise	SNC
Upper lobe							
Apicale							
Right	45/55	171.0±80.5	160.9±75.3	4.9±3.2	5.2±3.1	0.522	0.508
Left	NA*	NA	NA	NA	NA	—	—
Posterius							
Right	35/47	157.2±75.0	148.3±67.3	5.2±3.5	5.6±3.4	0.582	0.589
Left	57/59	156.9±71.4	132.8±62.9	5.0±3.1	5.6±3.5	0.05	0.35
Anterius							
Right	46/55	149.1±71.8	129.6±62.7	5.0±2.9	5.6±2.9	0.153	0.248
Left	37/41	142.3±55.7	125.8±56.2	5.3±2.5	6.4±2.7	0.199	0.059
Middle lobe							
Mediale	29/41	144.7±60.8	143.9±78.3	5.5±3.0	5.9±3.2	0.962	0.595
Laterale	43/53	154.0±67.3	135.8±60.9	5.2±3.5	5.8±3.3	0.169	0.42
Lingulare							
Superius	27/31	124.9±61.6	104.2±45.6	5.3±2.4	6.1±2.6	0.149	0.258
Inferius	42/52	147.8±70.7	130.1±64.5	5.2±2.8	6.2±2.7	0.208	0.156
Lower lobe							
Superius							
Right	57/71	144.1±59.9	141.7±65.5	5.5±3.8	6.0±4.1	0.834	0.474
Left	49/59	148.8±56.4	137.0±55.1	5.1±2.9	5.8±3.0	0.277	0.224
Basale anterius							
Right	42/49	148.1±69.1	130.8±73.8	5.0±2.8	5.2±2.7	0.252	0.751
Left	46/52	149.7±66.5	124.3±60.6	5.3±3.4	6.3±3.0	0.051	0.15
Basale mediale							
Right	31/35	155.4±64.0	152.8±62.6	5.0±3.0	5.4±2.8	0.87	0.664
Left	NA*	NA	NA	NA	NA	—	—
Basale lateral							

Right	44/56	154.1±65.0	143.6±58.3	5.1±2.9	5.4±3.1	0.399	0.554
Left	51/63	164.5±64.2	145.3±54.0	4.5±2.7	5.4±3.0	0.086	0.129
Basale posterius							
Right	54/69	158.9±62.2	146.9±58.1	5.1±2.7	5.5±3.5	0.271	0.504
Left	56/69	146.4±71.7	131.3±71.6	5.4±3.0	6.5±3.6	0.242	0.072

* NA are presented as not applicable. Data are mean ± SD, where *n* is the amount of the pulmonary lesions with available data. MP: Manual positioning; AP: AI-based positioning; SNR: Signal-to-noise ratio.

Table 3. Distribution of noise and SNR with MP and AP on particular lesion location at chest CT.

Lesion location	All lesions (*n*, MP/AP)	Noise		SNC		*P* value	
		MP	AP	MP	AP	Noise	SNC
Central	25/30	135.7±54.1	132.6±59.4	6.3±2.7	6.6±3.2	0.819	0.739
Peripheral	766/927	151.4±66.9	137.5±64.2	5.3±3.3	6.1±3.6	<0.001	<0.001

Data are mean ± SD, where *n* is the amount of the pulmonary lesions with available data. MP: Manual positioning; AP: AI-based positioning; SNR: Signal-to-noise ratio.

Figures

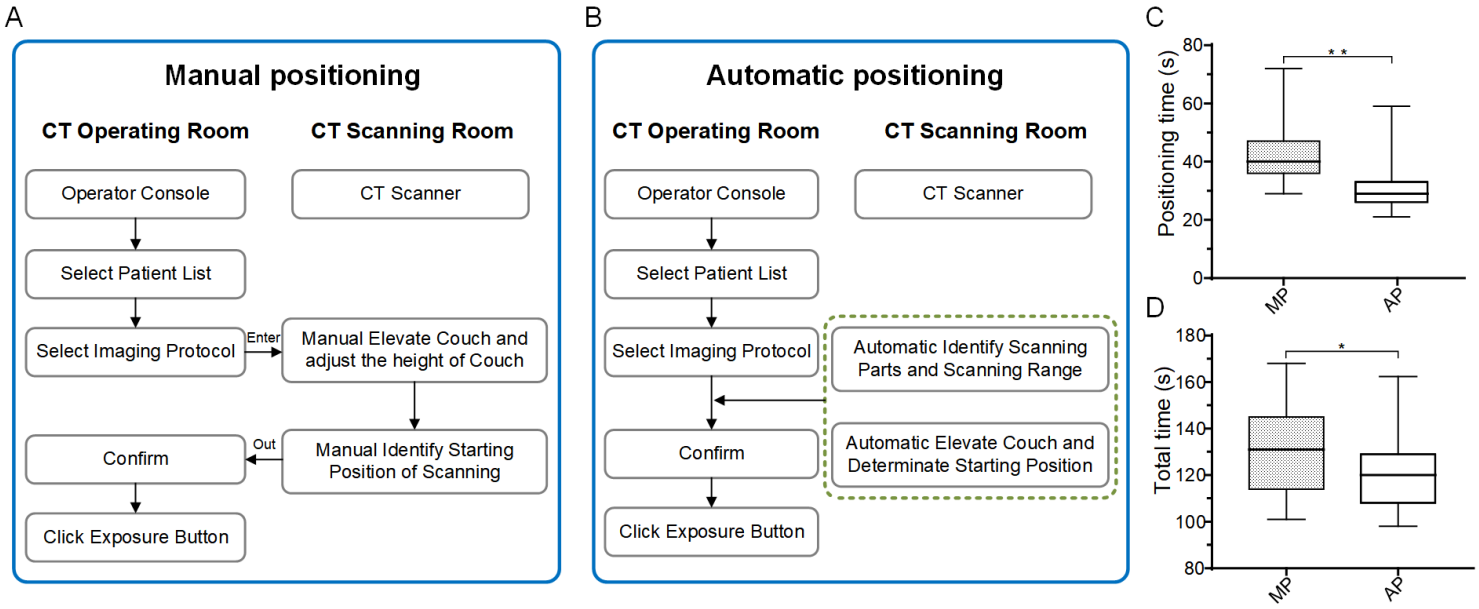

Figure 1

Schematic diagram for the operating steps of the manual positioning and automatic positioning. (A) Flowchart for the manual positioning. (B) Flowchart for the automatic positioning. (C) Quantification of total time. (D) Quantification of positioning time. Statistical p-values were calculated by a Wilcoxon signed-rank tests. In box plots, the central mark represents the median, and the edges of the box are the 25th and 75th percentiles. * denote $p < 0.05$, ** denote $p < 0.01$, n = 127 each.

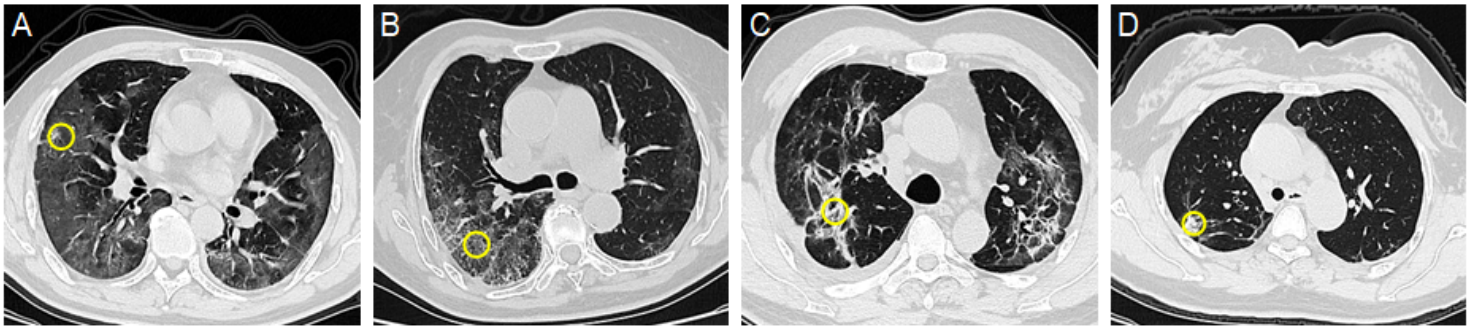

Figure 2

The measurement of CT value and noise on axial thin-section CT image in COVID-19 patients. Different types of lesions are shown along with ROI locations (yellow circles) used to acquire CT value measurements (mean ± SD) in different lung segments. (A) showing ground-glass opacification of lesions. (B) indicating thickened interlobular septa and intralobular interstitium (crazy-paving pattern). (C) showing linear opacities. (D) showing consolidation.

Figure 3

Positioning accuracy on chest CT topogram. (A) shows inaccurate chest topogram, in which lung field is incomplete displayed. (B) represents accurate chest CT topogram. (C) The positioning accuracy is comparable for chest topogram acquired by MP and AP. (Data were presented as n (%), where n was the number of patients with complete CT scout image; n = 127 each).

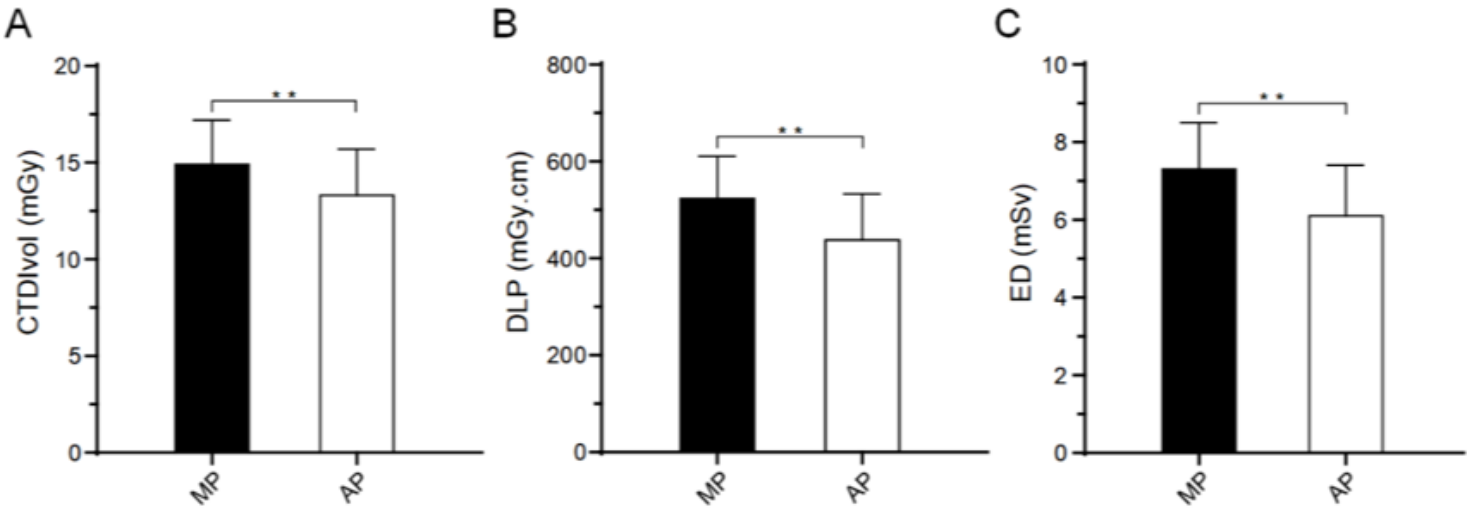

Figure 4

Impact of positioning mode on radiation dose of COVID-19 patients. (A) Volume CT dose index (CTDIvol) change of the patients after CT imaging with MP and AP mode. (B) shows dose length product (DLP) change. (C) shows effective dose (ED) change. (The values in the bar graph are given as the mean ± standard deviation (SD); ** denote $p < 0.001$; $n = 127$ each).

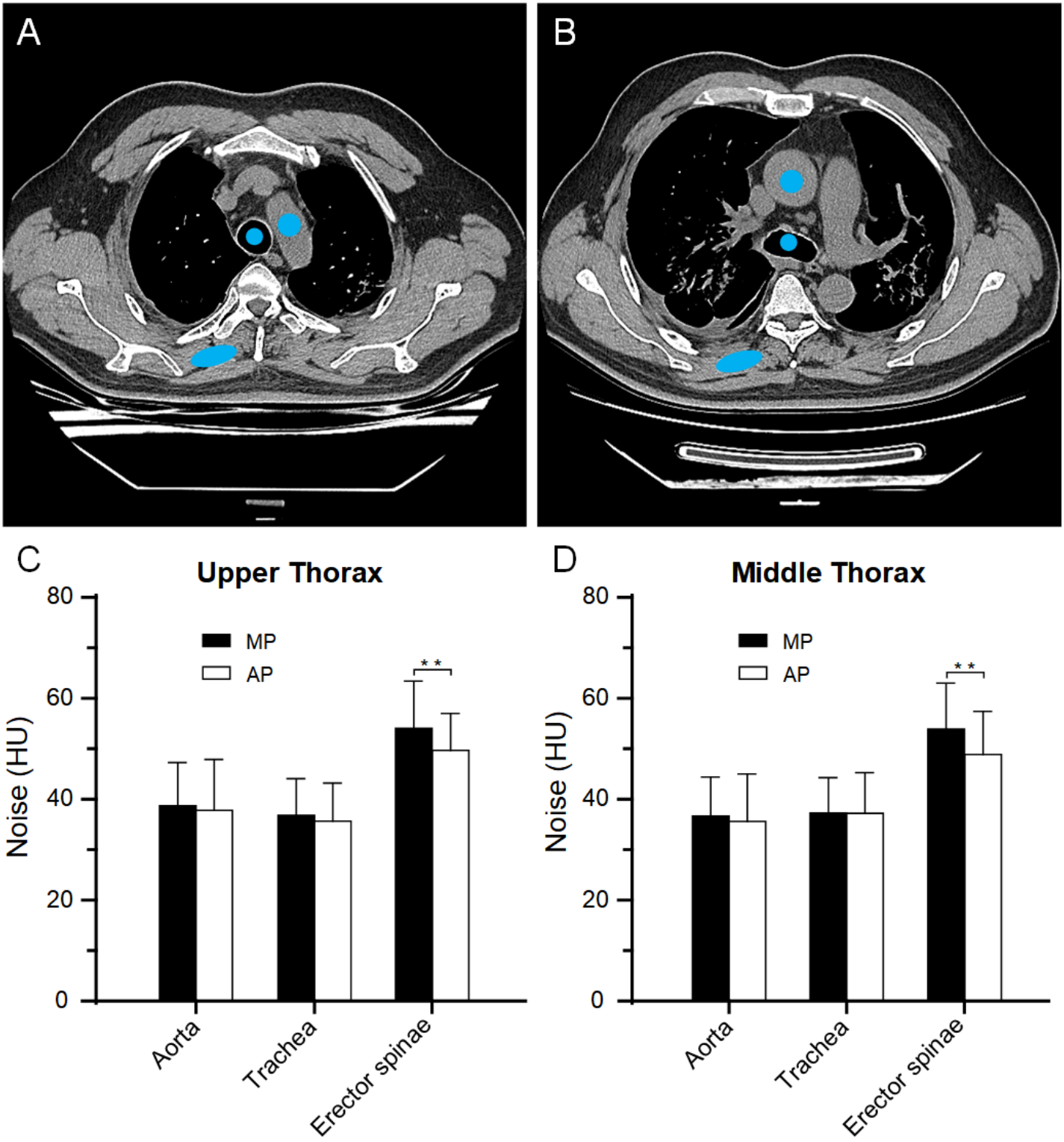

Figure 5

The influence of positioning mode on noise of chest CT images. Axial CT slices of upper thorax (A) and mid thorax (B) are shown along with ROI locations used to acquire CT value measurements (mean ± SD). the mean CT values and standard deviations (SDev) was calculated by drawing a 50 mm2 blue circles and blue oval ROI in a homogeneous-appearing area of aorta, trachea and erector spinae in the chest

area. (C) Comparison of noise on upper thorax. (D) Comparison of noise on middle thorax. (**p < 0.001 in paired-samples t tests; n = 127 each).

Supplementary Files

This is a list of supplementary files associated with this preprint. Click to download.

- SupplementaryFigure1.docx
- SupplementaryFigure2.docx